Molecular Pharmacology Fast Forward. Published on October 18, 2005 as doi:10.1124/mol.105.017210
This article has not been copyedited and formatted. The final version may differ from this version.

MOL 17210

Pharmacological profiling of *Orthochirus scrobiculosus* toxin 1 analogues with a trimmed N-terminal domain

Stéphanie Mouhat, Georgeta Teodorescu, Daniel Homerick, Violeta Visan, Heike Wulff, Yingliang Wu, Stephan Grissmer, Hervé Darbon, Michel De Waard and Jean-Marc Sabatier[#]

(S.M., J.-M.S.) Laboratoire Cellpep S.A., 13-15 Rue Ledru-Rollin, 13015 Marseille, France; CNRS Formation de Recherche en Evolution 2738, Boulevard Pierre Dramard, 13916 Marseille Cedex 20, France, (G.T., V.V., S.G.) Universität Ulm, Albert Einstein Allee 11, 89081 Ulm, Germany, (D.H., H.W.) Department of Medical Pharmacology and Toxicology, University of California, Davis, Davis CA 95616, U.S.A., (Y.W.) College of Life Sciences, Wuhan University, Wuhan, China, (H.D.) AFMB, CNRS UPR 9039, 31 Chemin Joseph Aiguier, 13402 Marseille, France, (M.D.W) INSERM U607, Département Réponse Dynamique et Cellulaire, 17 Rue des Martyrs, 38054 Grenoble Cedex 09, France; CEA, Grenoble, France ; Université Joseph Fourier, France.

Address correspondence to: Dr Jean-Marc Sabatier, CNRS Formation de Recherche en Evolution 2738, Boulevard Pierre Dramard, 13916 Marseille Cedex 20, France. Tel.: 33-4-91-69-88-52; Fax: 33-4-91-65-75-95; E-mail: sabatier.jm@jean-roche.univ-mrs.fr

Molecular Pharmacology Fast Forward. Published on October 18, 2005 as DOI: 10.1124/mol.105.017210
This article has not been copyedited and formatted. The final version may differ from this version.

Running title: Impact of trimming the N-terminus of an OSK1 analogue

Number of text pages: 23 pages

Number of figures: 6 figures and 1 table

Number of references: 25 references

Number of words: 162 in the Abstract, 484 in the Introduction, 1485 in the Results, and 504 in the Discussion.

The abbreviations used are: OSK1, toxin 1 from the scorpion *Orthochirus scrobiculosus*; AOSK1, [K^{16},D^{20}]-OSK1; [Δ^{1}]-AOSK1, AOSK1 deleted of the amino acid residue at position 1; [Δ^{1-4}]-AOSK1, AOSK1 deleted of the four N-terminal residues; [Δ^{1-6}]-AOSK1, AOSK1 deleted of the six N-terminal residues; [Δ^{1-7}]-AOSK1, AOSK1 deleted of the seven N-terminal residues; [Δ^{36-38}]-AOSK1, AOSK1 deleted of the last three C-terminal residues; [Δ^{1},T^{2}]-AOSK1, AOSK1 deleted of the amino acid residue at position 1 and mutated at position 2 by a Thr residue; Fmoc, N^{α}-fluoren-9-ylmethyloxycarbonyl; TFA, trifluoroacetic acid; MALDI-TOF, matrix-assisted laser-desorption ionization-time-of-flight; HPLC, high performance liquid chromatography; MS, mass spectrometry; 3-D, three-dimensional; IC_{50}, 50% inhibitory concentration; LD_{50}, 50% lethal dose; Kv, mammalian voltage-gated K^+ channels (Kv1.1 to Kv1.7); $K_{Ca}2.1$ (also referred to as SK1), type 1 small-conductance Ca^{2+}-activated K^+ channel; $K_{Ca}2.2$ (also referred to as SK2), type 2 small-conductance Ca^{2+}-activated K^+ channel; $K_{Ca}3.1$ (also referred to as IK1), type 1 intermediate-conductance Ca^{2+}-activated K^+ channels; $K_{Ca}1.1$ (also referred to as BK), large-conductance Ca^{2+}-activated K^+ channel; Kv11.1 (also referred to as HERG), human *ether-a-go-go* related K^+ channel; PDB, Protein Data Bank.

Molecular Pharmacology Fast Forward. Published on October 18, 2005 as DOI: 10.1124/mol.105.017210
This article has not been copyedited and formatted. The final version may differ from this version.

ABSTRACT

OSK1, a toxin from the venom of the Asian scorpion *Orthochirus scrobiculosus*, is a 38-residue peptide cross-linked by three disulfide bridges. A structural analogue of OSK1, [K^{16},D^{20}]-OSK1, was previously found to be one of the most potent blockers of the voltage-gated K^+ channel Kv1.3 hitherto characterized. Here, we demonstrate that progressive trimming of the N-terminal domain of [K^{16},D^{20}]-OSK1 results in marked changes in its pharmacological profile, in terms of both K^+ channel affinity and selectivity. While the affinity to Kv1.1 and Kv1.3 did not change significantly, the affinity to Kv1.2 and $K_{Ca}3.1$ was drastically reduced with the truncations. Surprisingly, a striking gain in potency was observed for Kv3.2. In contrast, a truncation of the C-terminal domain, expected to partially disrupt the toxin β-sheet structure, resulted in a significant decrease or a complete loss of activity on all channel types tested. These data highlight the value of structure-function studies on the extended N-terminal domain of [K^{16},D^{20}]-OSK1 to identify new analogues with unique pharmacological properties.

Molecular Pharmacology Fast Forward. Published on October 18, 2005 as DOI: 10.1124/mol.105.017210
This article has not been copyedited and formatted. The final version may differ from this version.

INTRODUCTION

OSK1 is a toxin that originates from the venom of the Asian scorpion *Orthochirus scrobiculosus* (Jaravine et al., 1997). It is composed of 38 amino acid residues with three disulfide bridges that are arranged according to a conventional pattern of the type C1-C4, C2-C5 and C3-C6 (Jaravine et al., 1997; Mouhat et al., 2004a; Mouhat et al., 2004b). OSK1, also referred to as α-KTx3.7, belongs to the α-KTx3 family (Tytgat et al., 1999; Rodriguez de la Vega and Possani, 2004) and shares between 74 and 90% sequence identity with other members of this family such as kaliotoxin 1 (Aiyar et al., 1995), agitoxins 1, 2 and 3 (Garcia et al., 1994) and *Buthus martensi* kaliotoxin (Romi-Lebrun et al., 1997). The 3-D solution structure of OSK1, as determined by ^{1}H-NMR (Protein Data Bank accession code 1SCO), indicates that the toxin folds according to the canonical α/β architectural motif which corresponds to a helical structure connected to an antiparallel β-sheet by two disulfide bridges (Jaravine et al., 1997; Mouhat et al., 2004b, Bontems et al., 1991). In the case of OSK1, the helical structure is a distorted α-helix running from amino acid residues 10 to 21, whereas the antiparallel β-sheet is composed of two strands going from residues 24 to 28 and 32 to 38. The N-terminal domain contains an extended structure (residues 2 to 6) resembling a third strand of the β-sheet.

OSK1 is a potent blocker of Kv1-family potassium channels, that targets Kv1.1 (IC_{50} value of 0.6 nM for current block), Kv1.2 (IC_{50} value of 5.4 nM) and Kv1.3 (IC_{50} value of 14 pM) with picomolar to nanomolar affinity. It is also moderately active on the calcium-activated K^+ channel $K_{Ca}3.1$ (IC_{50} value of 225 nM) (Mouhat et al., 2004b). Since OSK1 blocks both Kv1.3 and $K_{Ca}3.1$, two channels involved in the activation of human T and B cells (Chandy et al., 2004; Wulff et al., 2004), it constitutes a good lead compound for the development of new, OSK1-derived, immunosuppressive peptides of therapeutic value.

Molecular Pharmacology Fast Forward. Published on October 18, 2005 as DOI: 10.1124/mol.105.017210
This article has not been copyedited and formatted. The final version may differ from this version.

Recently, we reported the design and chemical production of an OSK1 analogue, [K^{16},D^{20}]-OSK1 (here referred to as AOSK1), that is about five times more potent on Kv1.3 (IC_{50} value of 3 pM) than OSK1 itself (Mouhat et al., 2004b). As such, AOSK1 is one of the most potent Kv1.3 channel blocker characterized so far. AOSK1 blocks $K_{Ca}3.1$ with roughly the same affinity as OSK1 itself, but displays a higher selectivity over Kv1.1 and Kv1.2. Here, this analogue was used as a template for the production and pharmacological characterization of a number of novel OSK1 analogues. Trimming of the N-terminal extended domain of AOSK1 specifically reduced the affinity to Kv1.2 and $K_{Ca}3.1$ but did not significantly change the affinity for Kv1.1 and Kv1.3. Unexpectedly, partial sequence trimming also proves to be a powerful approach to obtain AOSK1 analogues with pharmacological activities towards new K^+ channel subtypes such as Kv3.2.

Molecular Pharmacology Fast Forward. Published on October 18, 2005 as DOI: 10.1124/mol.105.017210
This article has not been copyedited and formatted. The final version may differ from this version.

MATERIALS AND METHODS

Materials - Fmoc-L-amino acids, 4-hydroxymethylphenyloxy (HMP) resin, and reagents used for peptide synthesis were obtained from PerkinElmer Life Sciences. Solvents were analytical grade products from SDS. L929, B82 and MEL cells stably expressing rat Kv1.2, mouse Kv1.3, human Kv1.5 and mouse Kv3.1 have been previously described (Grissmer et al., 1994). LTK (lacking leucocyte tyrosine kinase) cells expressing human Kv1.4 were obtained from Professor Michael Tamkun (Colorado State University, Fort Collins, CO, U.S.A.), CHO (Chinese-hamster ovary) cells expressing mouse Kv1.7 were from Vertex Pharmaceuticals (San Diego, CA, U.S.A.), HEK-293 (human embryonic kidney) cells expressing human $K_{Ca}1.1$ from Dr. Andrew Tinker (Centre for Clinical Pharmacology, University College London, London, U.K.), HEK-293 cells expressing human Kv11.1 (HERG) channel from Professor Craig T. January (Department of Medicine, University of Wisconsin, Madison, WI, U.S.A.), HEK-293 cells expressing human $K_{Ca}2.1$ and $K_{Ca}3.1$ from Dr. Khaled Houamed (University of Chicago, Chicago, IL, U.S.A.).

Production of AOSK1 Analogues by Solid-Phase Peptide Synthesis - AOSK1 was obtained as previously described (Mouhat et al., 2004b). The AOSK1 analogues ([Δ^1]-AOSK1, [Δ^{1-4}]-AOSK1, [Δ^{1-6}]-AOSK1, [Δ^{1-7}]-AOSK1, [Δ^{36-38}]-AOSK1 and [Δ^1,T^2]-AOSK1) were produced by chemical synthesis using a peptide synthesizer (Model 433A, Applied Biosystems Inc.). Peptide chains were assembled stepwise on 0.25 mmol of HMP resin (1% cross-linked; 0.65 mmol of amino group/g) using 1 mmol of Fmoc-L-amino acid derivatives (Merrifield, 1986). Side chain-protecting groups for trifunctional residues were: trityl for cysteine, asparagine, histidine and glutamine; *t*-butyl for serine, threonine, tyrosine, aspartate and glutamate; 2,2,4,6,7-pentamethyldihydrobenzofuran-5-sulfonyl for arginine; and *t*-butyloxycarbonyl for

Molecular Pharmacology Fast Forward. Published on October 18, 2005 as DOI: 10.1124/mol.105.017210
This article has not been copyedited and formatted. The final version may differ from this version.

lysine. N^{α}-amino groups were deprotected by successively treating with 18 and 20% (v/v) piperidine/N-methylpyrrolidone for 3 and 8 min, respectively. After three washes with *N*-methylpyrrolidone, the Fmoc-amino acid derivatives were coupled (20 min) as their hydroxybenzotriazole active esters in *N*-methylpyrrolidone (4-fold excess). After peptides were assembled, and removal of N-terminal Fmoc groups, the peptide resins (ca. 1.5 g) were treated under stirring for 3 h at 25°C with mixtures of TFA/H_2O/thioanisole/ethanedithiol (73:11:11:5, v/v) in the presence of crystalline phenol (2.1 g) in final volumes of 30 ml per gram of peptide resins. The peptide mixtures were filtered, precipitated and washed twice with cold diethyloxide. The crude peptides were pelleted by centrifugation (3,200 × g; 8 min). They were then dissolved in H_2O and freeze dried. Reduced AOSK1 analogues were solubilized at a concentration of ca. 0.6 mM in 0.2 M Tris-HCl buffer (pH 8.3) for oxidative folding (40 to 120 h depending on the peptide, 20°C). The folded/oxidized peptides were purified to homogeneity by reversed-phase high pressure liquid chromatography (HPLC) (C_{18} Aquapore ODS, 20 μm, 250 × 10 mm; PerkinElmer Life Sciences) by means of a 60-min linear gradient of 0.08% (v/v) TFA/H_2O (buffer A) with 0 to 40% of 0.1% (v/v) TFA/acetonitrile (buffer B), at a flow rate of 6 ml/min (λ = 230 nm). The purity and identity of each peptide were assessed by: (i) analytical C_{18} reversed-phase HPLC (C_{18} Lichrospher 5 μm, 4 × 200 mm; Merck) using a 60 min linear gradient of buffer A with 0-60% of buffer B, at a flow rate of 1 ml/min; (ii) amino acid analysis after peptide acidolysis [6 M HCl/2% (w/v) phenol, 20 h, 120°C, N_2 atmosphere]; and (iii) molecular mass determination by MALDI-TOF spectrometry.

Conformational analyses of AOSK1 analogues by one-dimensional ^{1}H-NMR - AOSK1 analogues were dissolved in a 9/1 mixture of H_2O/D_2O (v/v) at final concentrations of 50 μM. All ^{1}H-NMR measurements were performed on a BRUKER DRX 500 spectrometer equipped

Molecular Pharmacology Fast Forward. Published on October 18, 2005 as DOI: 10.1124/mol.105.017210
This article has not been copyedited and formatted. The final version may differ from this version.

with an HCN probe and self-shielded triple axis gradients were used. Experiments were performed at 300 K.

Lethality of AOSK1 analogues in mice - The peptides were evaluated for toxicity *in vivo* by determining the 50% lethal dose (LD_{50}) after intracerebroventricular injection into 20 g C57/BL6 mice (approved by the French ethics committee; animal testing agreement number 13.231 delivered by the Direction départementale des services vétérinaires des Bouches-du-Rhône (Préfecture des Bouches-du-Rhône, France)). Groups of six to eight mice per dose were injected with 5 µl peptide solution containing 0.1% (w/v) bovine serum albumin and 0.9% (w/v) NaCl.

Cell cultures and transfections - B82, MEL, L929 and HEK cells stably expressing the above mentioned voltage- and Ca^{2+}-activated K^+ channels and COS-7 cells used for transfection were maintained in DMEM with Earle's salts (Gibco, U.K.), and 10% heat-inactivated foetal calf serum (PAA, Austria) as previously described (Grissmer et al., 1994). Mouse Kv1.1 in a GFPIre vector (Invitrogen, Germany), human Kv1.2 in a pcDNA3/Hygro vector (Invitrogen, Germany) and rat Kv3.2 in a pcDNA3 vector (Protinac GmbH, Hamburg, Germany) were transfected into COS-7 cells either alone or with a GFP expressing construct using FuGene6 Transfection Reagent (Roche) according to the recommended protocol. Currents were recorded 1-3 days later in GFP-positive cells.

Electrophysiology - Electrophysiological experiments were carried out at 22-24^{o}C using the patch-clamp whole-cell recording mode (Hamill et al., 1981; Rauer and Grissmer, 1996). Cells were bathed with mammalian Ringer's solution (in mM): 160 NaCl, 4.5 KCl, 2 $CaCl_2$, 1 $MgCl_2$, and 10 HEPES (pH 7.4 with NaOH), with an osmolarity of 290-320 mOsm. When AOSK1 analogues were applied, 0.1% bovine serum albumin was added to the Ringer's solution. A syringe-driven perfusion device was used to exchange the external recording bath

Molecular Pharmacology Fast Forward. Published on October 18, 2005 as DOI: 10.1124/mol.105.017210
This article has not been copyedited and formatted. The final version may differ from this version.

solution. Two internal pipette solutions were used. One for measuring voltage-gated K^+ currents that contained (in mM): 155 KF, 2 $MgCl_2$, 10 HEPES, and 10 EGTA (pH 7.2 with KOH), with an osmolarity of 290-320 mOsm. Another for measuring Ca^{2+}-activated K^+ currents that contained (in mM): 135 K-aspartate, 8.7 $CaCl_2$, 2 $MgCl_2$, 10 EGTA, 10 HEPES (pH 7.2 with KOH), with an osmolarity of 290-320 mOsm. A free $[Ca^{2+}]_i$ of 1 μM was calculated. All currents through voltage-gated K^+ channels were elicited by 200 ms depolarising voltage steps from -80 to +40 mV. Potassium currents through $K_{Ca}1.1$, $K_{Ca}2.1$ and $K_{Ca}3.1$ were elicited by 1 μM internal $[Ca^{2+}]_i$ and 200 ms voltage ramps from -120 to 40 mV. Electrodes were pulled from glass capillaries (Science Products, Germany), and fire-polished to resistances of 2.5-5 MΩ. Membrane currents were measured with an EPC-9 or EPC-10 patch-clamp amplifier (HEKA Elektronik, Lambrecht, Germany) interfaced to a computer running acquisition and analysis software (Pulse and PulseFit). When voltage-gated K^+ currents were measured, the capacitive and leak currents were subtracted using a P/10 procedure. Series resistance compensation (> 80%) was used for currents above 2 nA. The holding potential was -80 mV in all experiments. Data analyses were performed with IgorPro (WaveMetrics, Oregon, USA), and IC_{50} values were deduced by fitting a modified Hill equation to the data ($I_{toxin}/I_{control} = 1/[1 + ([AOSK1\ analogue]/IC_{50})]$, where I is the peak current (for voltage-gated K^+ channels) or the slope of the ramp current (for Ca^{2+}-activated K^+ channels) to the normalized data points obtained with at least four different AOSK1 analogue concentrations.

RESULTS

Molecular Pharmacology Fast Forward. Published on October 18, 2005 as DOI: 10.1124/mol.105.017210
This article has not been copyedited and formatted. The final version may differ from this version.

Syntheses of AOSK1 analogues - A comparison of the amino acid sequences of OSK1, AOSK1 and its analogues is provided in Figure 1*a*. AOSK1 is an OSK1 analogue with two mutations in positions 16 (acidic Glu^{16} replaced by basic Lys) and 20 (basic Lys^{20} replaced by acidic Asp). While the net global charge of AOSK1 is the same as that of OSK1, the distribution of charged amino acid residues is different between the two compounds. A previous study had demonstrated that AOSK1 is a 5-fold more potent blocker of Kv1.3 than OSK1 (Mouhat et al., 2004b). AOSK1 is also more selective for Kv1.3 than OSK1. We therefore used it as a template for the rationale design of new structural analogues in which we trimmed either the N- or the C-terminus. In both cases, the number and relative positioning of all six half-cystine residues forming the three-disulfide bridges were preserved. The standard structural motif for the α/β scaffold in most scorpion toxins can be described by: $\mathbf{X}_n CX_n CX_3 CX_n (G/A/S) XCX_n CXC\mathbf{X}_n$ (where X represents an unspecified amino acid residue and *n* a variable number of residues). Bold $\mathbf{X}_n$ at N- and C-terminal extremities represent the residues that were selectively trimmed in the design of AOSK1 analogues. Using this approach, four N-terminal truncated AOSK1 analogues ([Δ^1]-AOSK1, [Δ^{1-4}]-AOSK1, [Δ^{1-6}]-AOSK1 and [Δ^{1-7}]-AOSK1) were chemically produced that shortened the N-terminal extended domain while keeping the first AOSK1 half-cystine residue intact. We further synthesized an analogue in which we truncated the first N-terminal amino acid residue (Gly^1) and mutated the second amino acid residue of AOSK1 from Val^2 to Thr ([Δ^1,T^2]-AOSK1). This point mutation was selected to produce an AOSK1 analogue possessing an N-terminal domain (i.e. TIINVK) that is identical to those of margatoxin and noxiustoxin, two scorpion toxins that potently block Kv1.3 (Possani et al., 1999; Rodriguez de la Vega et al., 2003). In addition, a C-terminal truncated AOSK1 analogue ([Δ^{36-38}]-AOSK1) was synthesized to evaluate the importance of this domain. The latter truncates half of the second strand (amino acid sequence 32 to 38) of the β-sheet structure, and we therefore expected it to show a

Molecular Pharmacology Fast Forward. Published on October 18, 2005 as DOI: 10.1124/mol.105.017210
This article has not been copyedited and formatted. The final version may differ from this version.

reduced potency because of the reported importance of the β-sheet structure for Kv channel blockage (Regaya et al., 2004). All the peptides were assembled by solid-phase synthesis using stepwise Fmoc/*t*-butyl chemistry, as described (Merrifield, 1986). After assembly, crude reduced peptides were obtained in yields ranging from 70 to 80%. The peptides were folded/oxidized under standard alkaline conditions, and purified by preparative C_{18} reversed-phase HPLC. Homogeneity of the purified peptides was > 99%, as assessed by analytical HPLC (Fig. 1*b*). Mass spectrometry analyses of the peptides using the MALDI-TOF technique gave experimental molecular masses similar to the deduced molecular masses (Fig. 1*c*), validating the identity of the desired products. All peptides were also characterized and quantified by amino acid analyses after acidolysis. A complete Edman sequencing was performed for some of them to further validate the final products (data not shown). The yield of peptide synthesis ranged between 1 and 5%.

Structural analysis of AOSK1 and truncated analogues by ^{1}H-NMR - One-dimensional ^{1}H-NMR was used to verify that the truncations did not generate unfolded species (Fig. 2). The well-dispersed signals of the amide regions suggest that the AOSK1 analogues are folded in compact conformations.

Comparison of lethal activities between AOSK1 and its analogues in mice - The synthetic peptides were compared for their lethal activities by intracerebroventricular injection in mice (Fig. 3). All peptides were lethal in mice with characteristic symptoms of K^+ channel-acting toxins, such as tremor, convulsions, and spasmic paralysis followed by death. The following order of *in vivo* lethality was observed (from the most to the least potent peptide): OSK1 > AOSK1 > [Δ^1]-AOSK1 = [Δ^1,T^2]-AOSK1 > [Δ^{1-4}]-AOSK1 > [Δ^{1-6}]-AOSK1 > [Δ^{1-7}]-AOSK1 >> [Δ^{36-38}]-AOSK1. The greatest difference in lethality between AOSK1 and [Δ^{1-7}]-AOSK1, its N-terminal most truncated analogue, is 6-fold. Interestingly, a good correlation seems to

Molecular Pharmacology Fast Forward. Published on October 18, 2005 as DOI: 10.1124/mol.105.017210
This article has not been copyedited and formatted. The final version may differ from this version.

exist between the size of the N-terminal truncation of AOSK1 and the resulting lethality of the AOSK1 peptides. This progressive decrease in lethality is thought to be associated with a decline in pharmacological potency towards vital K^+ channel subtype(s). In contrast, removal of the last three C-terminal AOSK1 residues (T^{36}, P^{37} and K^{38}) dramatically reduced toxicity and increased the LD_{50} value 16-fold compared to AOSK1. Accordingly, a previous structural characterization of OSK1 (Jaravine et al., 1997) revealed that T^{36} side-chain and K^{38} main chain mobility are important for the docking of OSK1 to K^+ channels.

Pharmacological activity of AOSK1 peptides on a large set of K^+ channel subtypes - The pharmacological profile of AOSK1 analogues was examined on ten voltage-gated and three Ca^{2+}-activated K^+ channel subtypes. None of the newly synthesized peptides (OSK1, AOSK1 and its analogues) showed any activity on either the voltage-gated channels Kv1.4, Kv1.5, Kv1.6, Kv1.7, Kv3.1 and Kv11.1 or the Ca^{2+}-activated K^+ channels $K_{Ca}1.1$ and $K_{Ca}2.1$ at micromolar concentrations. In contrast, the peptides inhibited the Kv-1 family channels Kv1.1, Kv1.2, Kv1.3, the Kv3-family channel Kv3.2 and the intermediate-conductance Ca^{2+}-activated K^+ channel $K_{Ca}3.1$ with varying potencies (Table 1). As illustrated in Table 1 and Figure 4, [Δ^{36-38}]-AOSK1 was the least effective of all analogues in blocking K^+ channel currents. This result agrees well with the observation that [Δ^{36-38}]-AOSK1 also shows the lowest activity when injected intracerebroventricular into mice (Fig. 3). However, [Δ^{36-38}]-AOSK1 low activity *in vitro* and *in vivo* was not unexpected since the integrity of the β-sheet structure has been reported to be crucial for the recognition of voltage-gated Kv and Ca^{2+}-activated $K_{Ca}3.1$ potassium channels by scorpion toxins (Castle et al., 2003; Rodriguez de la Vega et al., 2003; Regaya et al., 2004; Jouirou et al., 2004). In contrast, the most severe truncation of the N-terminal extended region of AOSK1 (i.e. [Δ^{1-7}]-AOSK1) produced differential effects depending on the subtype of K^+ channel (Fig. 4). AOSK1 activities on Kv1.1 and Kv1.3 currents were affected very little by the truncation of the last N-terminal

Molecular Pharmacology Fast Forward. Published on October 18, 2005 as DOI: 10.1124/mol.105.017210
This article has not been copyedited and formatted. The final version may differ from this version.

seven residues in [Δ^{1-7}]-AOSK1 as shown in the dose-response curves in Figure 4*b*. [Δ^{36-38}]-AOSK1 is shown for comparison. While [Δ^{1-7}]-AOSK1's potency in blocking Kv1.1 (IC_{50} value of 7.9 nM) and Kv1.3 (IC_{50} value of 114 pM) decreased only 20-38 fold, it was completely inactive on Kv1.2 currents at 1 μM (Fig. 4) translating into a more than 338-fold loss in activity. Since the truncation of entire N-terminal extended domain of AOSK1 in [Δ^{1-7}]-AOSK1 showed such a differential effect on the affinity to Kv1.1, Kv1.2 and Kv1.3, we next examined whether milder truncations of this N-terminal domain could preserve the drastic reduction of activity on Kv1.2 while generating analogues with better affinities for Kv1.1 and Kv1.3. Figure 5 shows the effects of a progressive trimming of the N-terminal domain on the IC_{50} values of the resulting AOSK1 analogues. The data demonstrate that N-terminal domain trimming reduces the potency of the compounds to block Kv1.2 much more than their potency to block Kv1.1 and Kv1.3. This observation indicates the greater importance of the N-terminal extended domain for Kv1.2 channel recognition by AOSK1. The [Δ^{1}]-AOSK1 analogue was of particular interest since it was 10- and 8-fold less potent on Kv1.2 and Kv1.3 but 2-fold more potent on Kv1.1 than AOSK1.

We further evaluated [Δ^{1},T^{2}]-AOSK1 since its N-terminal domain is identical to the Kv1.3 blocking scorpion toxins (α-KTx2.1 (noxiustoxin) and α-KTx2.2 (margatoxin)) (Tytgat et al., 1999, Rodriguez de la Vega et al., 2003). [Δ^{1},T^{2}]-AOSK1 was as potent as [Δ^{1}]-AOSK1 on Kv1.3, but its affinity further decreased by more than 3-fold for Kv1.2 as compared to [Δ^{1}]-AOSK1, to finally give a 34-fold difference in affinity for this channel compared to AOSK1. As such, [Δ^{1},T^{2}]-AOSK1 has a better selectivity than [Δ^{1}]-AOSK1 for Kv1.3. The N-terminal truncation strategy thus proves valuable for generating analogues with modified selectivity profiles and, possibly, with increased affinity towards specific channel subtype(s). Since AOSK1, but not OSK1, has a weak affinity for Kv3.2, we wondered whether any of the truncated AOSK1 analogues might be more potent Kv3.2 blockers than AOSK1. Fig. 6 illustrates that two analogues, [Δ^{1}]-AOSK1 and [Δ^{1},T^{2}]-AOSK1, are able to

Molecular Pharmacology Fast Forward. Published on October 18, 2005 as DOI: 10.1124/mol.105.017210
This article has not been copyedited and formatted. The final version may differ from this version.

block Kv3.2 currents more potently than AOSK1. The increases in affinity were 11- and 15-fold for [Δ^1]-AOSK1 and [Δ^1,T^2]-AOSK1, respectively. Further truncations of AOSK1 had the opposite effect and resulted in a complete loss of activity on Kv3.2, in line with observations made for other voltage-gated K^+ channels (Fig. 4).

Comparison for each peptide between IC_{50} values on individual channels and LD_{50} values indicates an interesting trend worth discussing. Briefly, it appears that the two most important channels for lethality in mouse brain are Kv1.1 and Kv1.2 as previously noticed (Mouhat et al., 2004b). It also appears that pharmacological activity on Kv3.2 is not essential for lethal potency. A tendency for a greater implication of Kv1.1 over Kv1.2 in the peptide-induced lethal effects is also evidenced. However, it should be noted that lethality probably involves other uncharacterized channels making such comparisons difficult.

DISCUSSION

The scorpion toxin OSK1 serves as a good lead for the design of new Kv1.3 channel blockers because of its potent action on this channel type, with an IC_{50} value of 14 pM. OSK1's ability to also block other voltage-gated K^+ channels such as Kv1.1 and Kv1.2 (in the low nanomolar concentration range) and one Ca^{2+}-activated K^+ channel ($K_{Ca}3.1$) with moderate activity (at high nanomolar concentration) means that the toxin displays an unusual wide range of channel targets. AOSK1 is an even more interesting lead for further derivatization because it is one of the most potent Kv1.3 channel blocker so far described (Middleton et al., 2003; Mouhat et al., 2004b). Compared to other published compounds acting on Kv1.3, AOSK1 displays specificity factors of 133 (over Kv1.1; see Table I) and 987 (over Kv1.2), which thus appears to be similar to ShK-Dap^{22} (Kalman et al., 1998), but better than ShK-F6CA (Beeton et al., 2003) or ShK(L5) (Beeton et al., 2005). Also, AOSK1 displays an even larger pharmacological profile through its additional action on Kv3.2. Therefore, AOSK1 is, to our knowledge, the second Kv3.2 channel blocker reported hitherto, after the sea anemone toxin

Molecular Pharmacology Fast Forward. Published on October 18, 2005 as DOI: 10.1124/mol.105.017210
This article has not been copyedited and formatted. The final version may differ from this version.

ShK acting in the low nanomolar concentration range (Yan et al., 2005). Here a strategy of domain trimming was used for the first time to generate new pharmacological profiles.

Several conclusions can be drawn from the experimental data obtained with these AOSK1 analogues. First, trimming in the C-terminal region of AOSK1 is expected to alter its β-sheet structure (Jaravine et al., 1997) and thereby reduces activity on all tested target channels. Second, trimming of the N-terminal region appears to be a more attractive strategy since the changes in activity differed greatly from one channel subtype to the other. Indeed, Kv1.1 and Kv1.3 channels were far less susceptible to decreases in analogue affinity than was Kv1.2. Interestingly, a limited trimming of the AOSK1 N-terminus turned out to be an interesting route for producing analogues with increased activity towards Kv3.2. We surmise that limited truncation may facilitate the access to the binding site of the peptides in the outer vestibule of the channel. As such, this indicates that some toxins can be inactive for a given channel type because of accessibility problems and, perhaps not, because they do not recognize a binding site on the channel. In future experiments, it will be of interest to combine various experimental strategies to obtain still more powerful toxin-derived drugs acting on specific voltage-gated and Ca^{2+}-activated potassium channels. In particular, structural determination and docking simulations of truncated AOSK1 peptides on the various target K^+ channels will be greatly helpful for this purpose. The challenge is to produce more selective AOSK1 analogues with high potencies on the Kv1.3 channel, with or without potent activity on $K_{Ca}3.1$ channel. Ultimately, such structure-function studies on AOSK1 may be useful for the production of potent immunosuppressive drugs. Combining N-terminal truncations with point mutations is clearly a powerful way to create new selective toxin-derived peptide blockers for Kv1.3, Kv1.1, $K_{Ca}3.1$ and Kv3.2 channels.

ACKNOWLEDGEMENTS

Molecular Pharmacology Fast Forward. Published on October 18, 2005 as DOI: 10.1124/mol.105.017210
This article has not been copyedited and formatted. The final version may differ from this version.

The authors wish to thank Dr. P. Mansuelle for Edman sequencing and amino acid analysis of AOSK1 peptides. Drs. B. De Rougé and E. Béraud are acknowledged for helpful discussions.

Molecular Pharmacology Fast Forward. Published on October 18, 2005 as DOI: 10.1124/mol.105.017210
This article has not been copyedited and formatted. The final version may differ from this version.

REFERENCES

Aiyar J, Withka JM, Rizzi JP, Singleton DH, Andrews GC, Lin W, Boyd J, Hanson DC, Simon M, Dethlefs B, Lee C, Hall JE, Gutman GA and Chandy KG (1995) Topology of the pore-region of a K^+ channel revealed by the NMR-derived structures of scorpion toxins. *Neuron* **15**:1169-1181.

Beeton C, Wulff H, Singh S, Botsko S, Crossley G, Gutman GA, Cahalan, MD, Pennington M and Chandy KG (2003) A novel fluorescent toxin to detect and investigate Kv1.3 channel up-regulation in chronically activated T lymphocytes. *J. Biol. Chem.* **278**: 9928-9937.

Beeton C, Pennington MW, Wulff H, Singh S, Nugent D, Crossley G, Khaytin I, Calabresi PA, Chen CY, Gutman GA and Chandy KG (2005) Targeting effector memory T cells with a selective peptide inhibitor of Kv1.3 channels for therapy of autoimmune diseases. *Mol. Pharmacol.* **67**: 1369-1381.

Bontems F, Roumestand C, Gilquin B, Ménez A and Toma F (1991) Refined structure of charybdotoxin: common motifs in scorpion toxins and insect defensins. *Science* **254**:1521-1523.

Castle NA, London DO, Creech C, Fajloun Z, Stocker JW and Sabatier JM (2003) Maurotoxin: a potent inhibitor of intermediate conductance Ca^{2+}-activated potassium channels. *Mol. Pharmacol.* **63**:409-418.

Chandy KG, Wulff H, Beeton C, Pennington M, Gutman GA and Cahalan MD (2004) K^+ channels as targets for specific immunomodulation. *Trends Pharmacol. Sci.* **25**:280-289.

Garcia ML, Garcia-Calvo M, Hidalgo P, Lee A and MacKinnon R (1994) Purification and characterization of three inhibitors of voltage-dependent K^+ channels from *Leiurus quinquestriatus* var. *hebraeus* venom. *Biochemistry* **33**:6834-6839.

Grissmer S, Nguyen AN, Aiyar J, Hanson DC, Mather RJ, Gutman GA, Karmilowicz MJ, Auperin AA and Chandy KG (1994) Pharmacological characterization of five cloned voltage-gated K^+ channels, types Kv1.1, 1.2, 1.3, 1.5, and 3.1, stably expressed in mammalian cell lines. *Mol. Pharmacol.* **45**:1227-1234.

Hamill OP, Marty A, Neher E, Sakmann B and Sigworth FJ (1981) Improved patch-clamp techniques for high-resolution current recording from cells and cell-free membrane patches. *Pflügers Arch.* **391**:85-100.

Jaravine VA, Nolde DE, Reibarkh MJ, Korolkova YV, Kozlov SA, Pluzhnikov KA, Grishin EV, and Arseniev AS (1997) Three-dimensional structure of toxin OSK1 from *Orthochirus scrobiculosus* scorpion venom. *Biochemistry* **36**:1223-1232.

Jouirou B, Mouhat S, Andreotti N, De Waard M and Sabatier JM (2004) Toxin determinants required for interaction with voltage-gated K^+ channels. *Toxicon* **43**:909-914.

Kalman K, Pennington MW, Lanigan MD, Nguyen A, Rauer H, Mahnir V, Paschetto K, Kem WR, Grissmer S, Gutman GA, Christian EP, Cahalan MD, Norton RS and Chandy KG (1998) ShK-Dap^{22}, a potent Kv1.3-specific immunosuppressive polypeptide. *J. Biol. Chem.* **273**:32697-32707.

Merrifield B (1986) Solid phase synthesis. *Science* **232**:341-347.

Middleton RE, Sanchez M, Linde AR, Bugianesi RM, Dai G, Felix JP, Koprak SL, Staruch MJ, Bruguera M, Cox R, Ghosh A, Hwang J, Jones S, Kohler M, Slaughter RS, McManus OW, Kaczorowski GJ and Garcia ML (2003) Substitution of a single residue in *Stichodactyla helianthus* peptide, ShK-Dap^{22}, reveals a novel pharmacological profile. *Biochemistry* **42**:13698-13707.

Mouhat S, Jouirou B, Mosbah A, De Waard M, and Sabatier JM (2004a) Diversity of folds in animal toxins acting on ion channels. *Biochem. J.* **378**:717-726.

Mouhat S, Visan V, Ananthakrishnan S, Wulff H, Andreotti N, Grissmer S, Darbon H, De Waard M, and Sabatier, JM (2004b) K^+ channel types targeted by synthetic OSK1, a toxin from *Orthochirus scrobiculosus* scorpion venom. *Biochem. J.* **384**:1-10.

Possani LD, Selisko B and Gurrola GB (1999) in *Perspectives in Drug Discovery and Design : Animal Toxins and Potassium Channels* (Darbon, H., and Sabatier, J. M., eds.) Vols. 15/16, pp. 15-40, Kluwer Academic Publishers, Dordrecht, The Netherlands.

Rauer H and Grissmer S (1996) Evidence for an internal phenylalkylamine action on the voltage-gated potassium channel Kv1.3. *Mol. Pharmacol.* **50**:1625-1634.

Regaya I, Beeton C, Ferrat G, Andreotti N, Darbon H, De Waard M and Sabatier JM (2004) Evidence for domain-specific recognition of SK and Kv channels by MTX and HsTx1 scorpion toxins. *J. Biol. Chem.* **279**:55690-55696.

Rodriguez de la Vega RC, Merino E, Becerril B and Possani LD (2003) Novel interactions between K^+ channels and scorpion toxins. *Trends Pharmacol. Sci.* **24**:222-227.

Rodriguez de la Vega RC and Possani LD (2004) Current views on scorpion toxins specific for K^+-channels. *Toxicon* **43**:865-875.

Romi-Lebrun R, Lebrun B, Martin-Eauclaire MF, Ishiguro M, Escoubas P, Wu FQ, Hisada M, Pongs O and Nakajima T (1997) Purification, characterization, and synthesis of three novel toxins from the Chinese scorpion *Buthus martensi*, which act on K^+ channels. *Biochemistry* **36**:13473-13482.

Tytgat J, Chandy KG, Garcia ML, Gutman GA, Martin Eauclaire MF, van der Walt JJ and Possani LD (1999) A unified nomenclature for short-chain peptides isolated from scorpion venoms: alpha-KTx molecular subfamilies. *Trends Physiol. Sci.* **20**:444-447.

Wulff H, Knaus HG, Pennington M and Chandy KG (2004) K^+ channel expression during B cell differentiation: implications for immunomodulation and autoimmunity. *J. Immunol.* **173**:776-786.

Yan L, Herrington J, Goldberg E, Dulski PM, Bugianesi RM, Slaughter RS, Banerjee P, Brochu RM, Briest BT, Kaczorowski GJ, Rudy B and Garcia ML (2005) *Stichodactyla helianthus* peptide, a pharmacological tool for studying Kv3.2 channels. *Mol. Pharmacol.* **67**:1513-1521.

Molecular Pharmacology Fast Forward. Published on October 18, 2005 as DOI: 10.1124/mol.105.017210
This article has not been copyedited and formatted. The final version may differ from this version.

FOOTNOTES

Address reprint requests to: Stéphanie Mouhat, CNRS Formation de Recherche en Evolution 2738, Boulevard Pierre Dramard, 13916 Marseille Cedex 20, France. Fax: 33-4-91-65-75-95; E-mail: stephanie_mouhat@yahoo.fr

Molecular Pharmacology Fast Forward. Published on October 18, 2005 as DOI: 10.1124/mol.105.017210
This article has not been copyedited and formatted. The final version may differ from this version.

LEGENDS OF FIGURES

Fig. 1. **Amino acid sequences and chemical syntheses of OSK1, AOSK1 and analogues thereof.** *a*, the amino acid sequences (one-letter code) of OSK1, AOSK1 and AOSK1 analogues were aligned according to the positions of their half-cystine residues (numbered from 1 to 6). The positions of half-cystine residues are highlighted in grey boxes. Mutated residues in AOSK1 (K^{16} and D^{20}) and related analogues are shown in bold. The positions of OSK1 secondary structures (an N-terminal extended domain located before the first half-cystine residue, an α-helix and a two-stranded β-sheet structure) are indicated by solid lines above the toxin amino acid sequence (1). The 3-D solution structure of OSK1 can be found in the PDB (code 1SCO). *b*, analytical C_{18} reversed-phase HPLC elution profiles of folded/oxidized OSK1, AOSK1 and its N- or C-terminal truncated analogues after their purification steps. *c*, deduced and experimental relative molecular masses $(M+H)^+$ of synthetic OSK1, AOSK1 and its analogues.

Fig. 2. **Structural analysis of AOSK1 peptides by ^{1}H-NMR.** One-dimensional ^{1}H-NMR spectra of AOSK1 and its truncated analogues. The spectrum of OSK1 is shown for comparison. Only the representative amide proton regions are shown. The overall distribution of resonance frequencies suggests that all peptides have similar global folds.

Fig. 3. **Lethal activities of AOSK1 and its analogues *in vivo* in mice.** LD_{50} values are provided in μg/kg. The LD_{50} value of OSK1 is indicated for comparison.

Fig. 4. **Block of K^+ channel subtypes by AOSK1, N-terminal truncated [Δ^{1-7}]-AOSK1 and C-terminal truncated [Δ^{36-38}]-AOSK1.** *a*, representative current traces in the absence (control) and presence (from left to right) of AOSK1, [Δ^{1-7}]-AOSK1 or [Δ^{36-38}]-AOSK1. The

concentration of applied peptide is provided on the figure. From top to bottom: representative Kv1.1, Kv1.2, Kv1.3 and $K_{Ca}3.1$ potassium currents. *b*, average normalized current inhibition by various concentrations of AOSK1 (open circles), [Δ^{1-7}]-AOSK1 (grey squares) or [Δ^{36-38}]-AOSK1 (filled diamonds) for each channel type (Kv1.1, Kv1.2, Kv1.3 and $K_{Ca}3.1$ channels, as indicated). Each data point represents the mean value ± S.D. of four experiments.

Fig. 5. **Impact of N- and C-terminal truncations on blocking potencies of AOSK1 towards Kv1.1, Kv1.2 and Kv1.3 channels.** AOSK1 *versus* its analogues: factors of increase in IC_{50} values for Kv1.1 (top), Kv1.2 (middle) and Kv1.3 channels (bottom). For each of these channel subtypes, the IC_{50} value of AOSK1 was normalized to 1 for the sake of comparison. The same scale was used for all three-channel types illustrating the more drastic effects of truncations on Kv1.2 current blockage.

Fig. 6. **Increased blocking potencies of [Δ^1]-AOSK1 and [Δ^1,T^2]-AOSK1 on Kv3.2 channel.** Representative current traces in the absence (control) and presence of OSK1, AOSK1, [Δ^1]-AOSK1, [Δ^1,T^2]-AOSK1, [Δ^{1-7}]-AOSK1 or [Δ^{36-38}]-AOSK1. The concentration of applied peptide is provided on each panel. Note that (i) OSK1 is inactive on Kv3.2 at micromolar concentration contrary to AOSK1, and (ii) [Δ^1]-AOSK1 and [Δ^1,T^2]-AOSK1 are more potent than AOSK1 on Kv3.2 channel.

IC_{50} values of AOSK1 peptides on various K^+ channel subtypes.

	OSK1	AOSK1	[Δ^1]-AOSK1	[Δ^1,T^2]-AOSK1	[Δ^{1-4}]-AOSK1	[Δ^{1-6}]-AOSK1	[Δ^{1-7}]-AOSK1	[Δ^{36-38}]-AOSK1
LD_{50} (µg/kg)	2	2.5	3	3	5	6.5	15	40
IC_{50} (nM)								
Kv1.1	0.60 ± 0.04	0.40 ± 0.01	0.19 ± 0.01	0.36 ± 0.04	2.67 ± 0.50	2.18 ± 0.30	7.90 ± 1.20	365 ± 65
Kv1.2	5.40 ± 1.89	2.96 ± 0.01	30 ± 7	100 ± 5	245 ± 77	634 ± 5	ne	ne
Kv1.3	0.014 ± 0.001	0.003 ± 0.001	0.025 ± 0.002	0.021 ± 0.004	0.038 ± 0.001	0.045 ± 0.002	0.114 ± 0.005	1.85 ± 0.70
Kv3.2	ne	1000 ± 100	95 ± 10	65 ± 10	ne	ne	ne	ne
K_{Ca}3.1	225 ± 10	228 ± 92	425 ± 25	ne	ne	ne	ne	ne
Specificity factor								
Kv1.3 *vs* Kv1.1	43	133	8	17	70	48	69	197
Kv1.3 *vs* Kv1.2	386	987	1200	4762	6447	14089	nd	nd
Kv1.1 *vs* Kv1.2	9	7	158	2778	92	291	nd	nd

For each peptide, the IC_{50} value is provided in nanomolar concentration. Data for OSK1 are shown for comparison. No effects (ne) of the peptides were observed for Kv1.4, Kv1.5, Kv1.6, Kv1.7, Kv3.1, Kv11.1, K_{Ca}1.1 and K_{Ca}2.1 at micromolar concentrations. Specificity factors (the ratios between IC_{50} values for two channels) are shown for the sake of comparison. nd, not determined.

Molecular Pharmacology Fast Forward. Published on October 18, 2005 as DOI: 10.1124/mol.105.017210
This article has not been copyedited and formatted. The final version may differ from this version.

Fig. 1

a

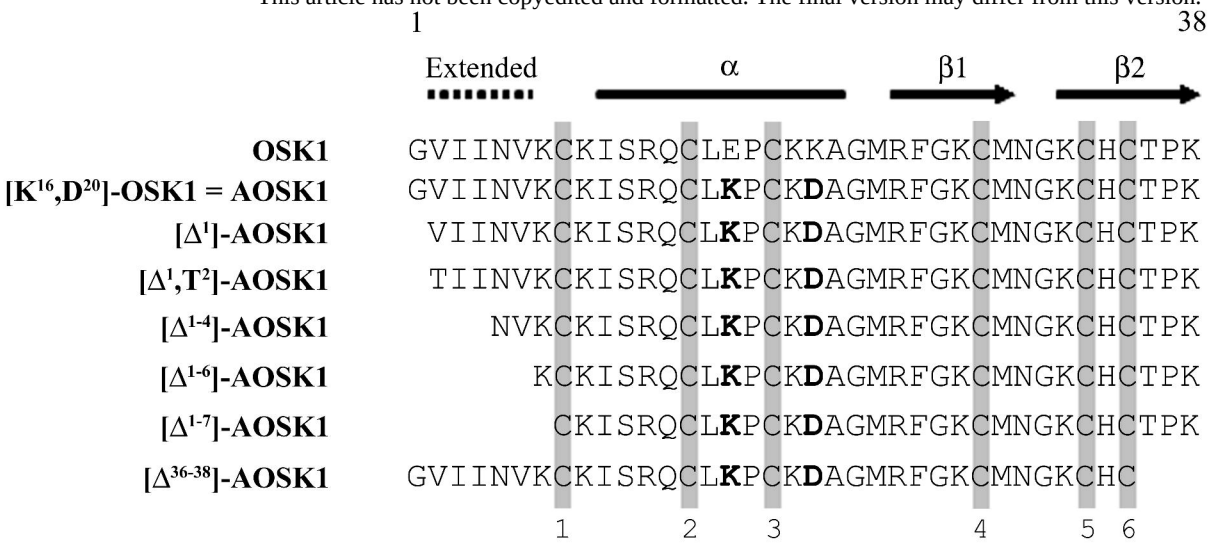

b

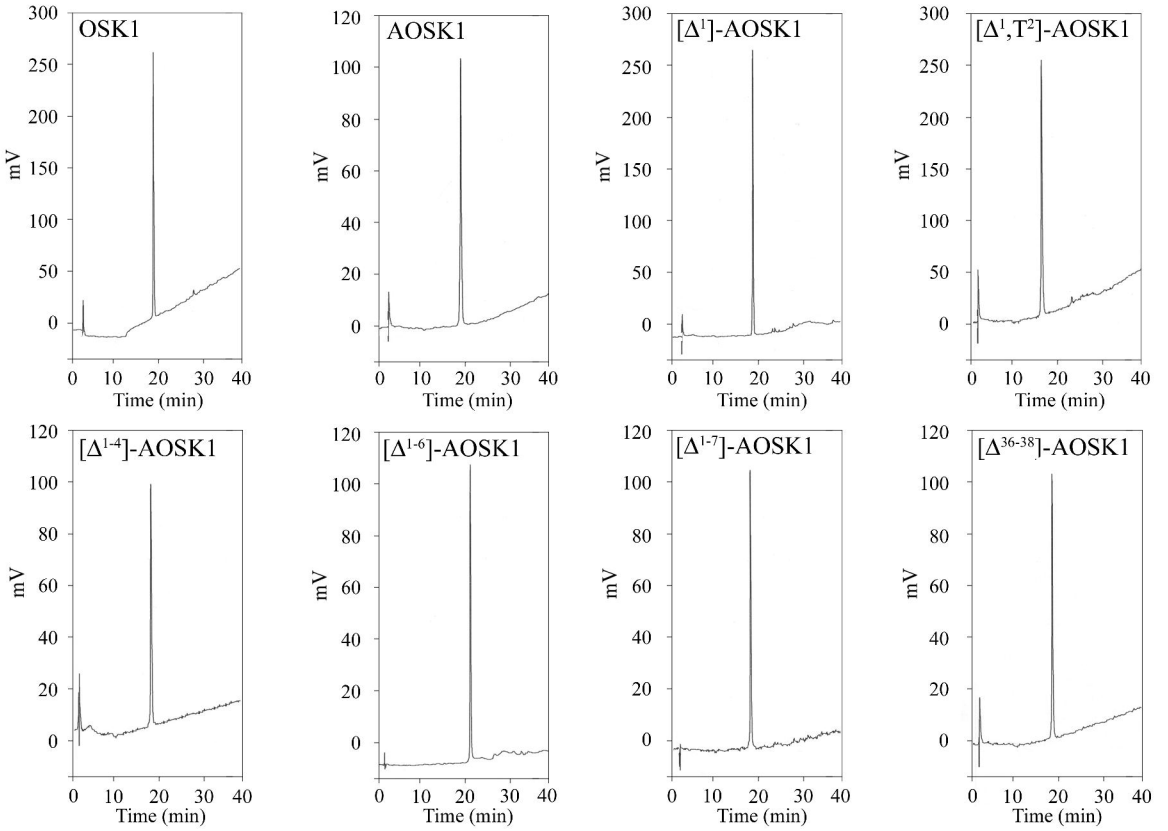

c

Peptide	Deduced Mr $(M+H)^+$	Experimental Mr $(M+H)^+$
OSK1	4206.2	4206.6
AOSK1	4192.2	4193.0
[Δ1]-AOSK1	4135.2	4135.6
[Δ1,T2]-AOSK1	4137.1	4137.4
[Δ1–4]-AOSK1	3809.7	3809.9
[Δ1–6]-AOSK1	3596.5	3596.9
[Δ1–7]-AOSK1	3468.3	3468.7
[Δ36–38]-AOSK1	3865.8	3866.5

Fig. 2

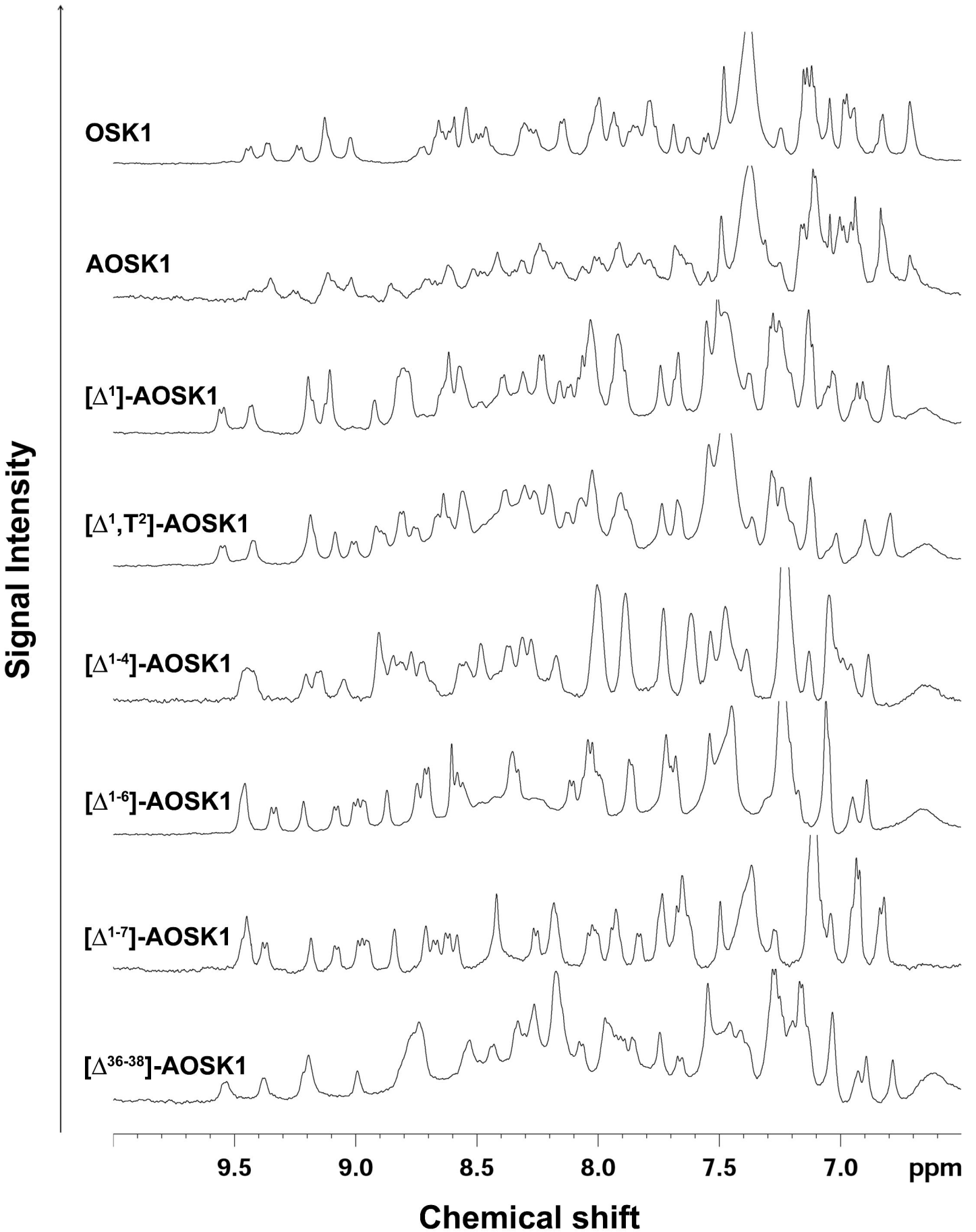
OSK1
AOSK1
[Δ1]-AOSK1
[Δ1,T2]-AOSK1
[Δ1-4]-AOSK1
[Δ1-6]-AOSK1
[Δ1-7]-AOSK1
[Δ36-38]-AOSK1
Signal Intensity
9.5
9.0
8.5
8.0
7.5
7.0
ppm
Chemical shift

Molecular Pharmacology Fast Forward. Published on October 18, 2005 as DOI: 10.1124/mol.105.017210

Fig. 3

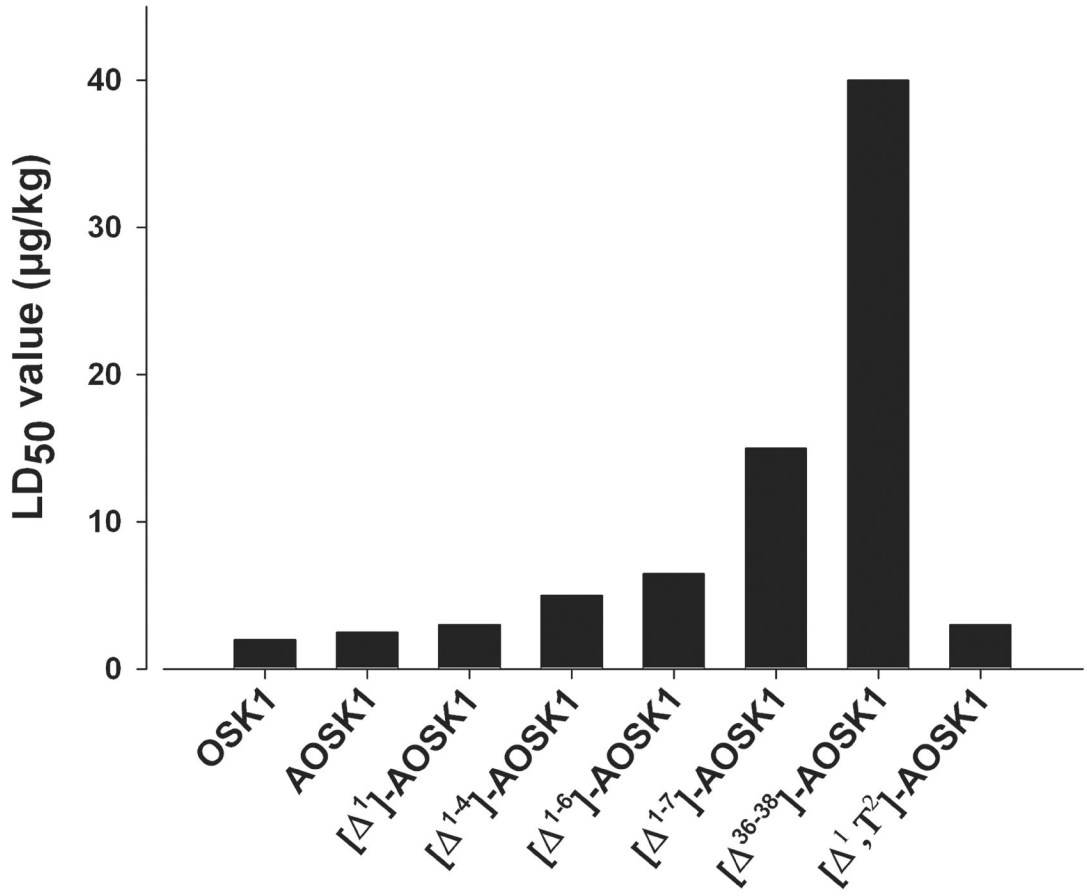

Molecular Pharmacology Fast Forward. Published on October 18, 2005 as DOI: 10.1124/mol.105.017210
This article has not been copyedited and formatted. The final version may differ from this version.

Fig. 4

a

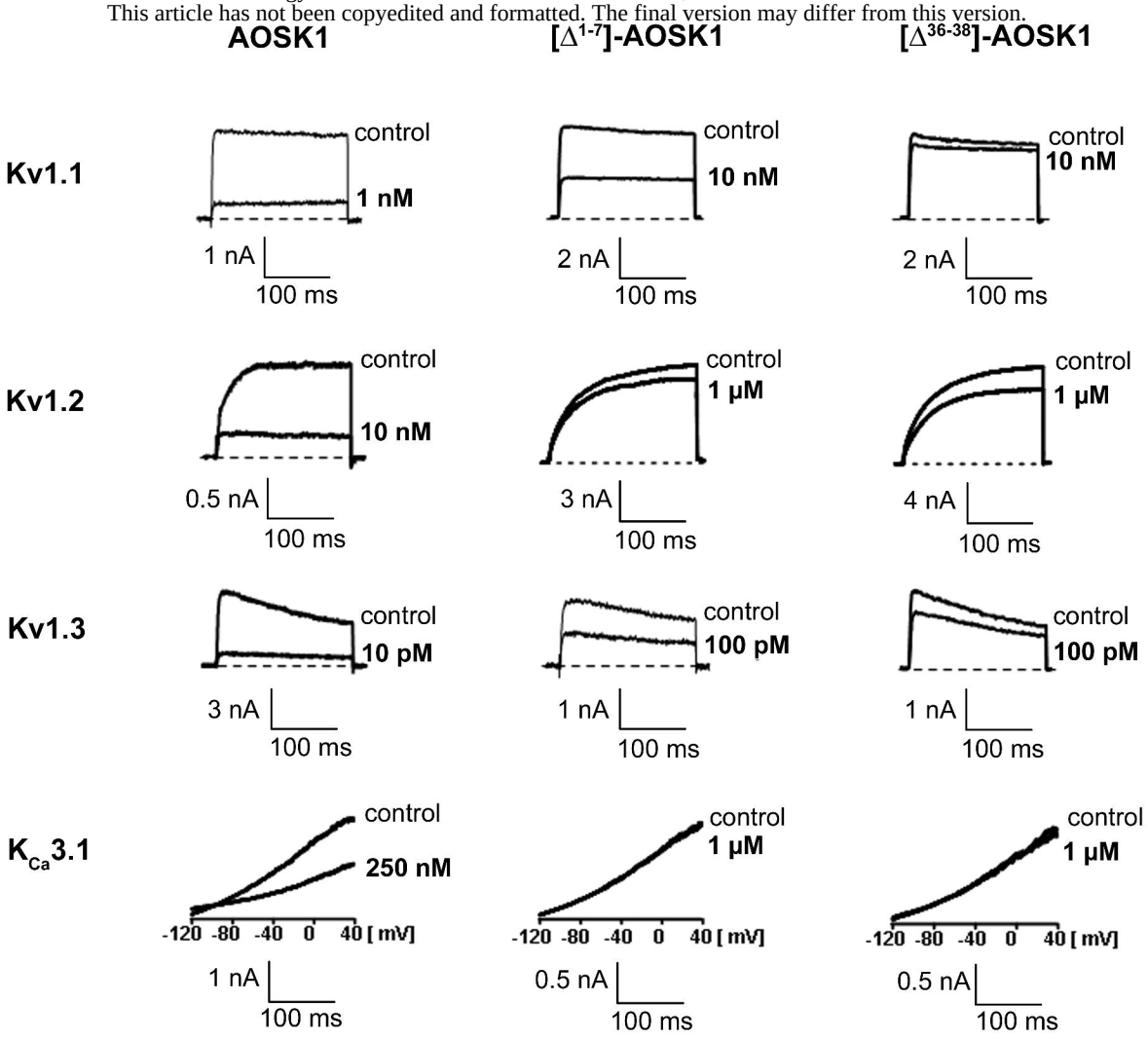

b

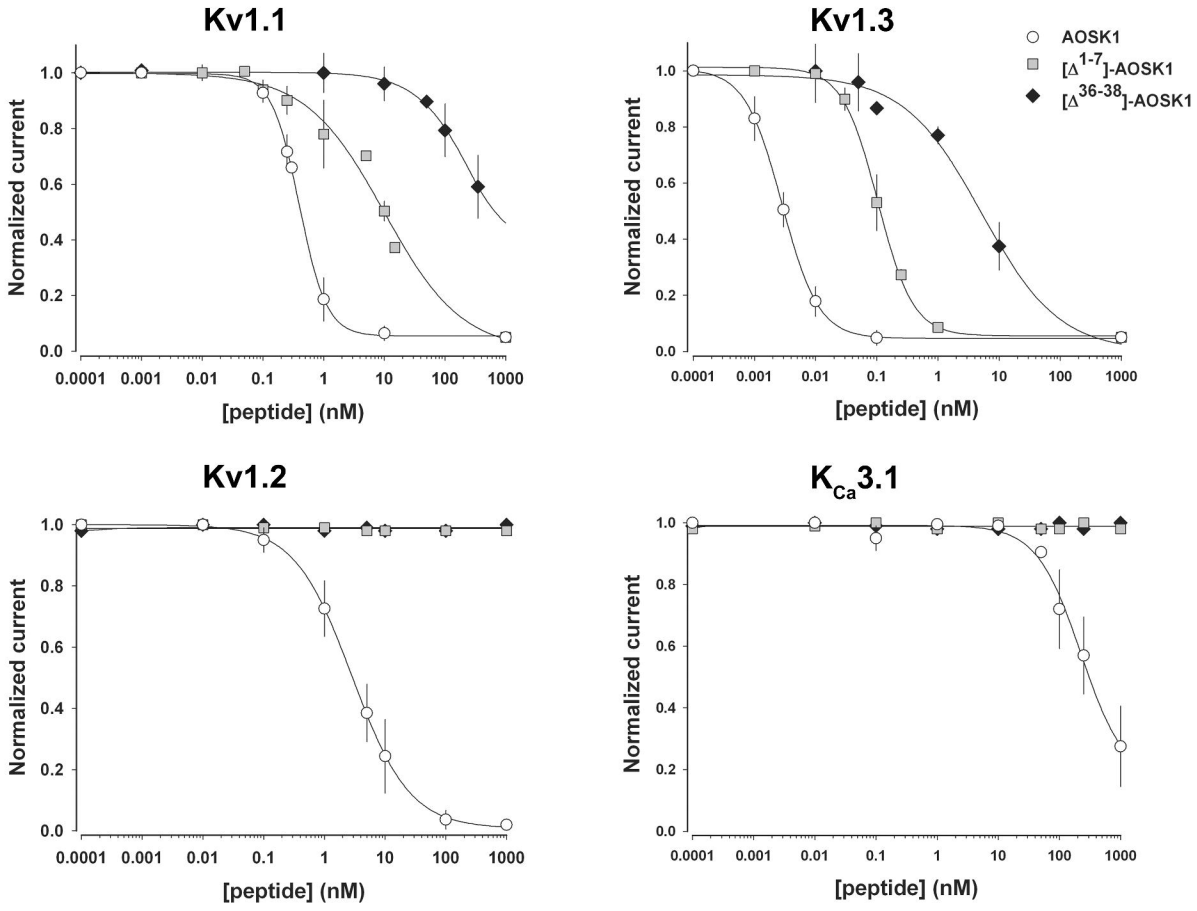

Molecular Pharmacology Fast Forward. Published on October 18, 2005 as DOI: 10.1124/mol.105.017210
This article has not been copyedited and formatted. The final version may differ from this version.

Fig. 5

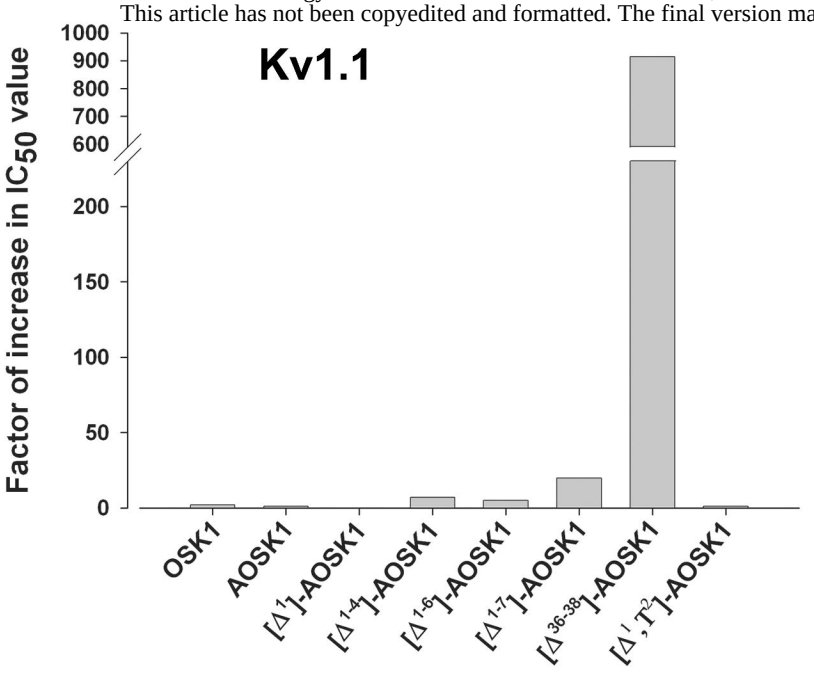

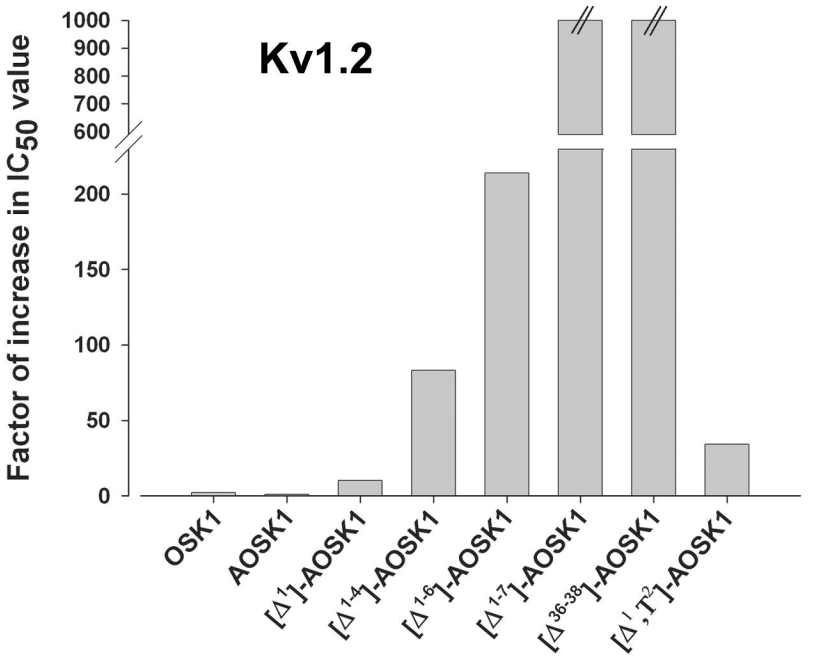

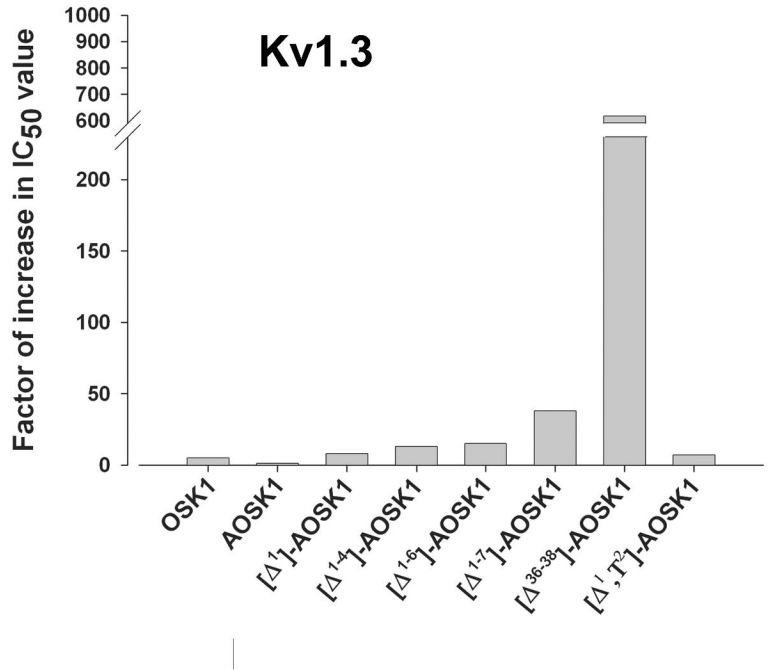

Fig. 6